Cell Research (2013) 23:1356-1368.
© 2013 IBCB, SIBS, CAS All rights reserved 1001-0602/13 $ 32.00
www.nature.com/cr

ORIGINAL ARTICLE

miR-142-3p regulates the formation and differentiation of hematopoietic stem cells in vertebrates

Xinyan Lu[1, *], Xiajuan Li[1, *], Qiuping He[1], Jiao Gao[2], Ya Gao[1], Bing Liu[2], Feng Liu[1]

[1]*State Key Laboratory of Biomembrane and Membrane Biotechnology, Institute of Zoology, Chinese Academy of Sciences, Beijing 100101, China;* [2]*307-Ivy Translational Medicine Center, Laboratory of Oncology, Affiliated Hospital of Academy of Military Medical Sciences, Beijing 100071, China*

Previous studies on developmental hematopoiesis have mainly focused on signaling and transcription factors, while the appreciation of epigenetic regulation including that of microRNAs is recent. Here, we show that in zebrafish and mouse, *miR-142-3p* is specifically expressed in hematopoietic stem cells (HSCs). Knockdown of *miR-142a-3p* in zebrafish led to a reduced population of HSCs in the aorta-gonad-mesonephros (AGM) region as well as T-cell defects in the thymus. Mechanistically, *miR-142a-3p* regulates HSC formation and differentiation through the repression of *interferon regulatory factor 7* (*irf7*)-mediated inflammation signaling. Finally, we show that *miR-142-3p* is also involved in the development of HSCs in mouse AGM, suggesting that it has a highly conserved role in vertebrates. Together, these findings unveil the pivotal roles that *miR-142a-3p* plays in the formation and differentiation of HSCs by repressing *irf7* signaling.

***Keywords*:** hematopoietic stem cell; *miR-142a-3p*; *irf7*; zebrafish; mouse

Cell Research (2013) **23**:1356-1368. doi:10.1038/cr.2013.145; published online 29 October 2013

Introduction

Genetic control over the development of hematopoietic stem cells (HSCs) is highly conserved in vertebrates, thus allowing the use of model organisms, such as zebrafish and mouse, to elucidate the regulatory mechanisms underlying HSC programming [1, 2]. In zebrafish, HSCs emerge from the ventral wall of the dorsal aorta via an endothelial-to-hematopoietic transition (EHT) [3, 4], migrate to the caudal hematopoietic tissue (CHT) and finally home to the thymus and kidney to produce T cells and other blood cell lineages [2]. The self-renewal and differentiation of HSCs ensure a lifelong supply of hematopoietic cells to meet the demand and to renew blood cells in organs, which must be tightly controlled at the cellular and molecular levels. However, the underlying molecular mechanisms of HSC specification and differentiation during vertebrate embryogenesis are still poorly understood.

microRNAs (miRNAs) are a group of non-coding RNAs (~22 nt) that can silence gene expression by binding to the 3′ untranslated region (UTR) or to the coding region of target mRNAs to promote mRNA destabilization or inhibit protein translation [5, 6]. Importantly, many miRNAs have been shown to be expressed in hematopoietic lineages and to act as pivotal regulators of transcriptional programs for normal hematopoiesis, including HSC self-renewal, differentiation and functioning [7, 8]. For example, *miR-126* is highly expressed in human and mouse HSCs, and the attenuation of *miR-126* activity by lentivirus-mediated knockdown leads to the inexhaustible expansion of HSCs *in vivo* in mouse and human [9]. Zebrafish *miR-126* was reported to be necessary for the precise regulation of the erythroid/megakaryocytic lineage choice during definitive hematopoiesis *in vivo* [10]. In addition, *miR-144* and *miR-451*, as direct targets of the critical hematopoietic master regulator GATA1, are required for erythropoiesis in zebrafish and mouse [11-13]. *miR-142-3p* is an evolutionally conserved miRNA of vertebrates, which is expressed in many different hematopoietic cells [14-21]. Chen *et al*.

*These two authors contributed equally to this work.
Correspondence: Feng Liu
Tel: +86 (10) 64807307; Fax: +86 (10) 64807313
E-mail: liuf@ioz.ac.cn
Received 16 July 2013; revised 19 August 2013; accepted 17 September 2013; published online 29 October 2013

[15] first reported that *miR-142* is expressed in embryonic and adult hematopoietic tissues, including the fetal liver, bone marrow, spleen and thymus, in mice, indicating its role in both embryonic and adult hematopoiesis. Later studies using mouse and human cell lines have indicated that *miR-142-3p* is required for the development and function of terminally differentiated hematopoietic lineages, such as myeloid and dendritic cells. *miR-142-3p* can directly regulate the expression of *tab2* in the myeloid lineage [22] and that of *IL-6* in dendritic cells(DCs) [23]. Very recently, zebrafish *miR-142-3p* (ZFIN ID: ZDB-GENE-090929-151, *miR-142a-3p* herein) has been shown to be required for the maturation of primitive erythrocytes, cardiogenesis and vessel integrity [24, 25]. However, the mechanisms underlying miRNA regulation of HSC development *in vivo* during vertebrate embryogenesis remain largely unclear.

Here, we show that in zebrafish, *miR-142a-3p* controls HSC specification and differentiation by suppressing the expression of *interferon regulatory factor 7* (*irf7*), revealing the pivotal roles of *miR-142a-3p* in HSC development. Moreover, *miR-142-3p* is also involved in the development of HSCs in mouse aorta-gonad-mesonephros (AGM) both *in vitro* and *in vivo*, suggesting that it has a well-conserved role in vertebrates.

Results

miR-142-3p is evolutionarily conserved and expressed in HSCs during zebrafish embryogenesis

miR-142-3p is highly conserved in vertebrates, from zebrafish to mammals (Supplementary information, Figure S1A). During zebrafish embryogenesis, *miR-142a-3p* expression was detected by RT-PCR from the tailbud stage onward (Supplementary information, Figure S1B). Whole mount *in situ* hybridization (WISH) showed that *miR-142a-3p* is expressed at low levels in the AGM region at 24 hour post fertilization (hpf), where the first HSCs will emerge 6-10 h later [3] (Figure 1A). Using the transgenic *runx1*:EGFP (Zhang P and Liu F, unpublished data) and *cmyb*:EGFP [26] lines, *miR-142a-3p* was found to be highly expressed in GFP-positive cells, which rep-

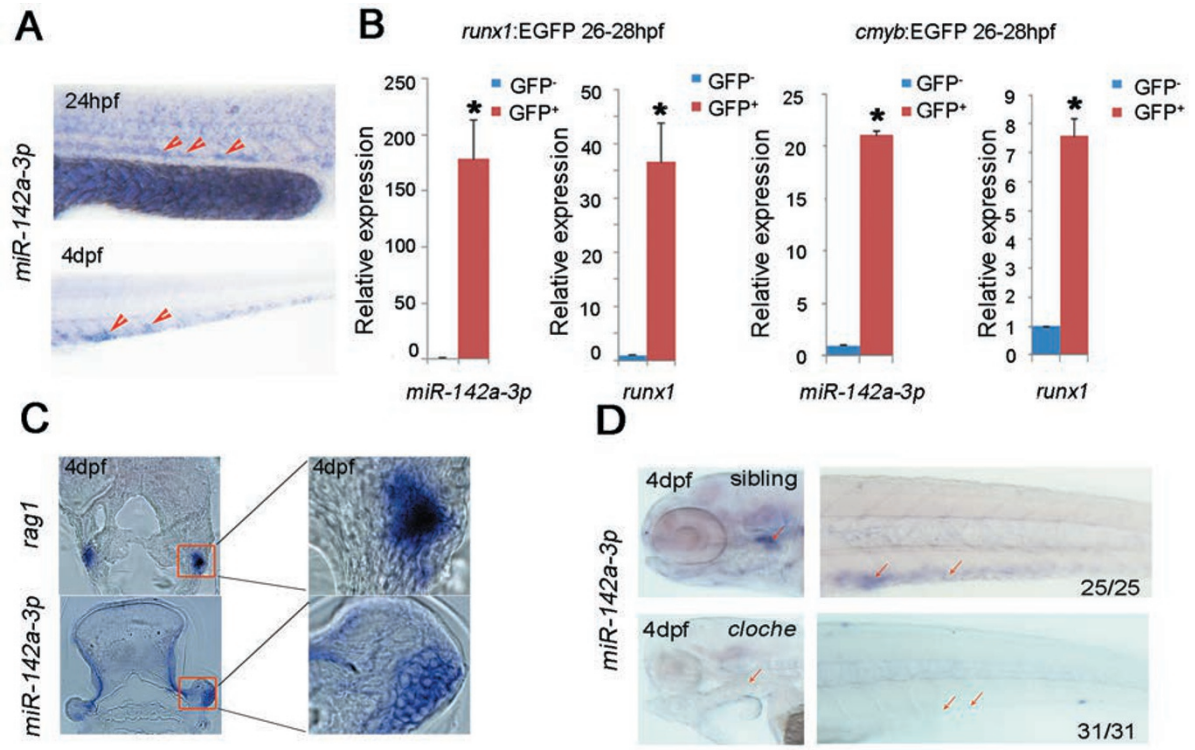

Figure 1 *miR-142a-3p* is specifically expressed in HSCs and T cells in zebrafish. **(A)** WISH images showing *miR-142a-3p* expression in the AGM (red arrowheads) at 24 hpf and in the CHT (red arrowheads) at 4 dpf. **(B)** qPCR results showing the expression of *miR-142a-3p* in sorted *runx1*:EGFP- or *cmyb*:EGFP-positive HSCs vs EGFP-negative cells. *runx1* was used as a positive control. **(C)** Frozen sections showing the expression of *rag1* and *miR-142a-3p* in the thymus at 4 dpf. The red square marks the thymus region. **(D)** WISH images showing the absence of *miR-142a-3p* expression in the thymus and CHT of the *cloche* mutants compared with WT siblings at 4 dpf.

resent the population of hematopoietic stem/progenitor cells, at 26-28 hpf (Figure 1B). Starting from 48 hpf and onwards, *miR-142a-3p* was specifically expressed in the CHT and at 4 day post fertilization (dpf) in the thymus (Figure 1A and 1C). Immunostaining of cryosections of 4 dpf embryos further confirmed that *miR-142a-3p* was expressed in the thymus (Figure 1C). In contrast, the expression of *miR-142a-3p* was not detected in either the thymus or the CHT region of *cloche* mutants that lack hematopoietic cells (Figure 1D), indicating that *miR-142a-3p* is indeed expressed in hematopoietic cells. The specific hematopoietic expression of *miR-142a-3p* suggests that it might play a critical role in definitive hematopoiesis.

Loss of miR-142a-3p leads to defects in HSC development and T-cell differentiation

To interrogate the function of *miR-142a-3p*, we analyzed the effects of blocking the formation of mature *miR-142a-3p* by using two different antisense morpholinos (MOs) targeting different sites of the *miR-142a-3p* stem loop, *3p* MO1 and *3p* MO2, and a mismatch morpholino of *miR-142a-3p*, *mis 3p* MO, was used as a control (Figure 2A and Supplementary information, Table S1). To exclude the possibility that developmental delay was caused by the morpholino injections, we examined the expression of the somite marker *myod* and found that its expression levels were not obviously different in the controls and morphants at 24 hpf (Supplementary information, Figure S2A). Additionally, the expression of the neuron and pronephric duct marker *pax2.1* was also not altered (Supplementary information, Figure S2A). These data suggest that at 24 hpf, the morphants grew relatively normally after the *miR-142a-3p* knockdown. qPCR showed that the endogenous expression of *miR-142a-3p* was reduced to various degrees (2-7 folds) by *3p* MO1 or *3p* MO2 injection (at 3.2 ng per embryo) (Figure 2A). WISH using a locked nucleic acid (LNA) antisense probe against mature *miR-142a-3p* revealed that the expression of *miR-142a-3p* in the thymus and the CHT was almost undetectable in the *miR-142a-3p* morphants and that the suppression effect continued through 4 dpf (Supplementary information, Figure S2B and S2C). Thus, the hematopoietic expression of *miR-142a-3p* was efficiently suppressed by both MOs (Figure 2A, Supplementary information, Figure S2B and S2C). Interestingly, the expression of *miR-142a-5p*, which originates from the opposite strand of the *miR-142a* gene, was detectable only in the thymus but not in the AGM region, and its expression in the thymus was also reduced by both of the *miR-142a-3p* MOs (data not shown).

To test whether *miR-142a-3p* influences HSC development and differentiation, we examined the expression of multiple markers of HSCs and hematopoietic lineages, such as the HSC genes *runx1* and *cmyb* and the T-cell markers *rag1* and *ikaros*. The WISH and qPCR results showed that the *miR-142a-3p* morphants (generated by injection of *3p* MO1 or *3p* MO2) displayed decreased expression of *runx1* and *cmyb* in the AGM and CHT at various stages (Figure 2B, 2C and Supplementary information, Figure S3A), whereas the *miR-142a-5p* knockdown did not have any effect on *runx1* expression in the AGM (data not shown), suggesting that *miR-142a-3p*, but not *miR-142a-5p*, is required for HSC development in zebrafish. Moreover, at 4 dpf, the expression of the T-cell markers *rag1* and *ikaros* was also decreased, whereas the expression of the thymic epithelial cell markers *foxn1* and *ccl25a* remained unchanged (Figure 2E, 2F and Supplementary information, Figure S3A-S3C), suggesting that the decrease in the T-cell population resulting from the loss of *miR-142a-3p* expression is not attributable to a defective thymic epithelial microenvironment. Furthermore, knockdown experiments performed using the *cmyb*:EGFP transgenic line showed that the *miR-142a-3p* morphants had significantly reduced *cmyb*$^+$ HSC populations in both the AGM and CHT regions (Figure 2D). In contrast, embryos injected with mismatch MOs displayed normal expression of the HSC markers *runx1* and *cmyb*, and the T-cell marker *rag1* (Figure 2B, 2C and Supplementary information, Figure S3A). To further confirm that the defects in HSC development in the morphants truly resulted from *miR-142a-3p* knockdown, we tested whether a *miR-142a-3p* duplex can rescue HSC gene expression in the *miR-142a-3p* morphants. Indeed, WISH showed that the decreased *runx1* expression in the morphants was rescued by the duplex (Figure 2G). Time-course analysis revealed the continuous decrease in *cmyb* expression in the AGM and CHT of the morphants from 36 hpf to 5 dpf (Supplementary information, Figure S3D), further supporting that this defect in HSC development in the *miR-142a-3p* morphants was not due to developmental delay. Together, these data demonstrate that *miR-142a-3p* is required for HSC development and T-cell differentiation.

Hemogenic endothelium but not arterial programming is affected in miR-142a-3p morphants

The decreased expression of the HSC master regulators *runx1* and *cmyb* in the *miR-142a-3p* morphants indicates that HSC emergence and development were severely disrupted. The first HSCs emerge in the ventral wall of the dorsal aorta (i.e., the hemogenic endothelium) via an EHT process, and arterial specification is a prerequisite for the normal emergence of HSCs [1]. To test whether the arterial programming was affected, we examined the expression of the arterial marker *dltC* and

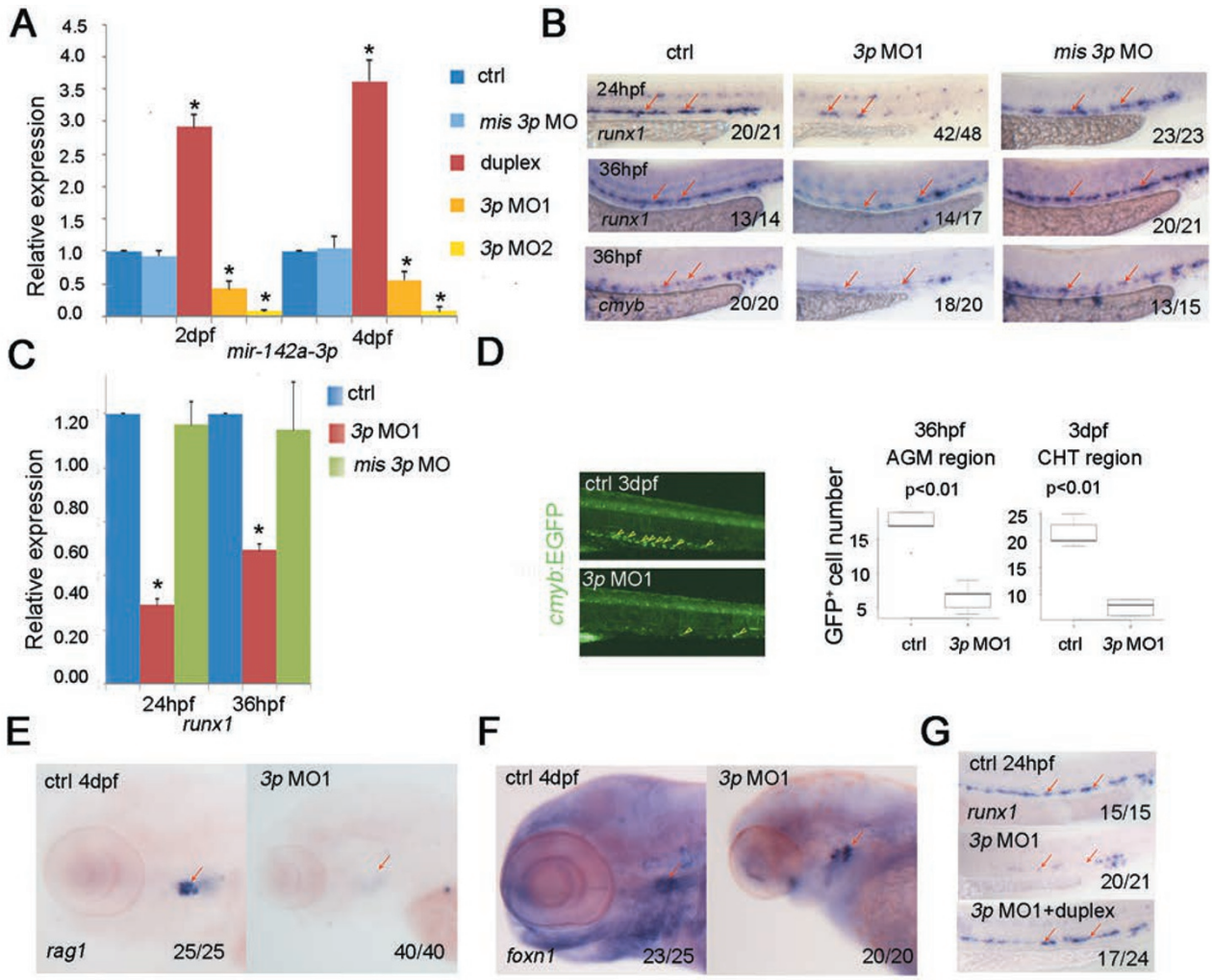

Figure 2 Loss of *miR-142a-3p* leads to defects in HSC development and T-cell differentiation in zebrafish. **(A)** Expression of *miR-142a-3p* in embryos injected with the *miR-142a-3p* mismatch MO, duplex, or two different *miR-142a-3p* MOs, at 2 and 4 dpf (mean ± SD, *t*-test, **P* < 0.05, *n* = 3). Total RNA extracted from embryos at 2 and 4 dpf was subjected to qPCR, with *U6* serving as the internal control. **(B)** WISH images showing the decreased expression of the HSC master regulators *runx1* and *cmyb* in *miR-142a-3p* morphants, but no changes in the embryos injected with *mis 3p* MOs. **(C)** qPCR results showing the decreased *runx1* expression in *miR-142a-3p* morphants, but no changes in embryos injected with *mis 3p* MOs at 24 and 36 hpf (mean ± SD, *t*-test, **P* < 0.05, *n* = 3). **(D)** *miR-142a-3p* knockdown in *cmyb*:EGFP transgenic zebrafish embryos led to a decreased *cmyb*$^+$ population. Left panel, representative fluorescence images showing the *cmyb*$^+$ population in the CHT at 3 dpf. Right panels, quantitative analyses of the *cmyb*$^+$ populations in the AGM (36 hpf) and CHT (3 dpf), showing a significant difference between the *miR-142a-3p* morphants and the controls (mean ± SD, *t*-test, *P* < 0.01, *n* = 3). **(E)** Decreased expression of the T-cell marker *rag1* in *miR-142a-3p* morphants at 4 dpf. The red arrows indicate the thymus. **(F)** Unchanged expression of the thymic epithelial cell marker *foxn1* in *miR-142a-3p* morphants at 4 dpf. The red arrows indicate the thymus. **(G)** Restoration of *runx1* expression by *miR-142a-3p* duplex in *miR-142a-3p* morphants at 24 hpf. The red arrows indicate the HSCs in the AGM region.

the venous marker *flt4* using WISH. The results showed that the expression of *dltC* and *flt4* was unchanged in the morphants (Figure 3A), suggesting that arterial/venous programming is not disrupted. Furthermore, a *3p* MO1 injection experiment using *fli1a*:EGFP transgenic zebrafish showed that the dorsal aorta is normal in the morphants, compared with that of the controls (Figure 3B).

The decrease of *runx1* expression at 24 hpf in the AGM region of *miR-142a-3p* morphants (Figure 2B and Supplementary information, Figure S3A) indicated that the specification of the hemogenic endothelium might be affected. To verify this hypothesis, we used the double-

transgenic line *kdrl*:mCherry/*cmyb*:EGFP in which the double-positive cells (yellow cells) represent hemogenic endothelial cells [4]. Indeed, at 36 hpf, the number of *kdrl*$^+$*cmyb*$^+$ cells was reduced in the *miR-142a-3p* morphants, which persisted until 60 hpf, the latest stage that we monitored (Figure 3C). The reduction of the hemogenic endothelial cell population was unlikely due to dysregulated cell proliferation or cell-cycle arrest (data not shown). Therefore, considering the high expression of *miR-142a-3p* in the sorted *cmyb*$^+$ or *runx1*$^+$ cells at 26-28 hpf in wild-type (WT) zebrafish (Figure 1B), and the decrease of *runx1* expression at 24 hpf (Figure 2B and Supplementary information, Figure S3A) as well as the reduced number of *kdrl*$^+$*cmyb*$^+$ cells at 36 hpf in *miR-142a-3p* morphants (Figure 3C), we concluded that the *miR-142-3p* knockdown affected hemogenic endothelial specification, which in turn attenuated the emergence of the earliest HSCs in the embryos.

Expression profiling identified downstream targets of miR-142a-3p

Direct comparison of the global gene expression patterns between control and *miR-142a-3p*-knockdown embryos might reveal further clues toward elucidating the biological effects of *miR-142a-3p* on HSC formation and differentiation. To identify the direct downstream targets of *miR-142a-3p*, we performed a combination of microarray, RT-PCR and miRNA target prediction (Figure 4A-4C and Supplementary information, Figure S4). The total RNAs of the AGM region in controls and *miR-142a-3p* morphants at both 2 dpf and 4 dpf were extracted and reverse-transcribed. The Cy3- or Cy5-labeled cDNAs were hybridized to a zebrafish oligo microarray. Gene set enrichment analysis was applied to the gene expression data to identify *miR-142a-3p*-modulated signaling and gene expression (Figure 4A). In total, 70 genes were up-regulated at both 2 dpf and 4 dpf (Figure 4B). Based on combined target-prediction analyses using Pictar and TargetScan, four potential *miR-142a-3p* targets, *irf7*, *krt18*, *foxp1a* and *rxrab* were further analyzed in detail using RT-PCR, qPCR and WISH (Supplementary information, Figure S4A-S4C). The results showed that among these four genes, the expression of *irf7* was dramatically up-regulated in *miR-142a-3p* morphants compared to controls (Supplementary information, Figure S4A and S4B), suggesting that *irf7* may be a primary target of *miR-142a-3p* in HSCs and their differentiated lineages. Although *irf7* is one of the components of interferon signaling, its role in HSC development has not been reported. Therefore, we chose *irf7* for functional analysis.

irf7 is a direct target of miR-142a-3p

irf7 has an imperfect match with *miR-142a-3p*, which

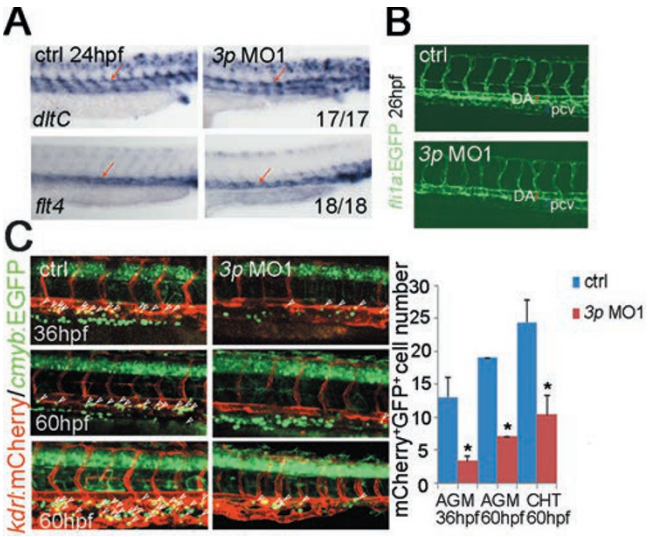

Figure 3 Loss of *miR-142-3p* did not affect artery/vein identity, but affected hemogenic endothelial specification. **(A)** WISH images showing the unchanged expression of arterial marker *dltC* and venous marker *flt4* in *miR-142a-3p* morphants at 24 hpf. **(B)** Confocal microscopy showing the unaffected artery and vein development in *miR-142a-3p* morphants using *fli1a*:EGFP transgenic zebrafish. DA, dorsal aorta. **(C)** Decreased number of hemogenic endothelial cells in the AGM as well as decreased HSCs in the CHT of *miR-142a-3p* morphants produced using the *kdrl*:mCherry/*cmyb*:EGFP transgenic line. Right panel, quantitative analyses of the *kdrl*$^+$/*cmyb*$^+$ populations showed a significant difference between the *miR-142a-3p* morphants and the controls (mean ± SD, *t*-test, $^*P < 0.05$, $n = 3$).

potentially targets residues 312 to 339 of the *irf7* 3′ UTR (with a minimum free energy (MFE) of –24.3 kcal/mol; RNAHybrid Website: http://bibiserv.techfak.uni-bielefeld.de/rnahybrid/), but has no match with *miR-142a-5p* (Figure 4C and data not shown). qPCR results showed that *irf7* expression level was markedly increased in the *miR-142a-3p* morphants at 2 dpf and 4 dpf (Supplementary information, Figure S4B). To determine whether *miR-142a-3p* regulates *irf7* expression directly or indirectly, we fused the zebrafish *irf7* 3′ UTR containing the putative *miR-142a-3p* recognition site or mutated sites (mu1 or mu2) with a luciferase reporter (Figure 4D), and transfected the reporter together with the *miR-142a-3p* duplex into HEK293T cells. Luciferase activity was strongly repressed when *miR-142a-3p* was co-expressed with the WT pGL3-*irf7*-3′ UTR but not when it was co-expressed with the mutant ones (Figure 4E). Western blotting showed that the expression level of *irf7* was decreased in duplex-injected embryos (Figure 4F). Taken together, these results suggest that *miR-142a-3p* directly binds to the *irf7* 3′ UTR region in a sequence-specific manner to repress *irf7* expression.

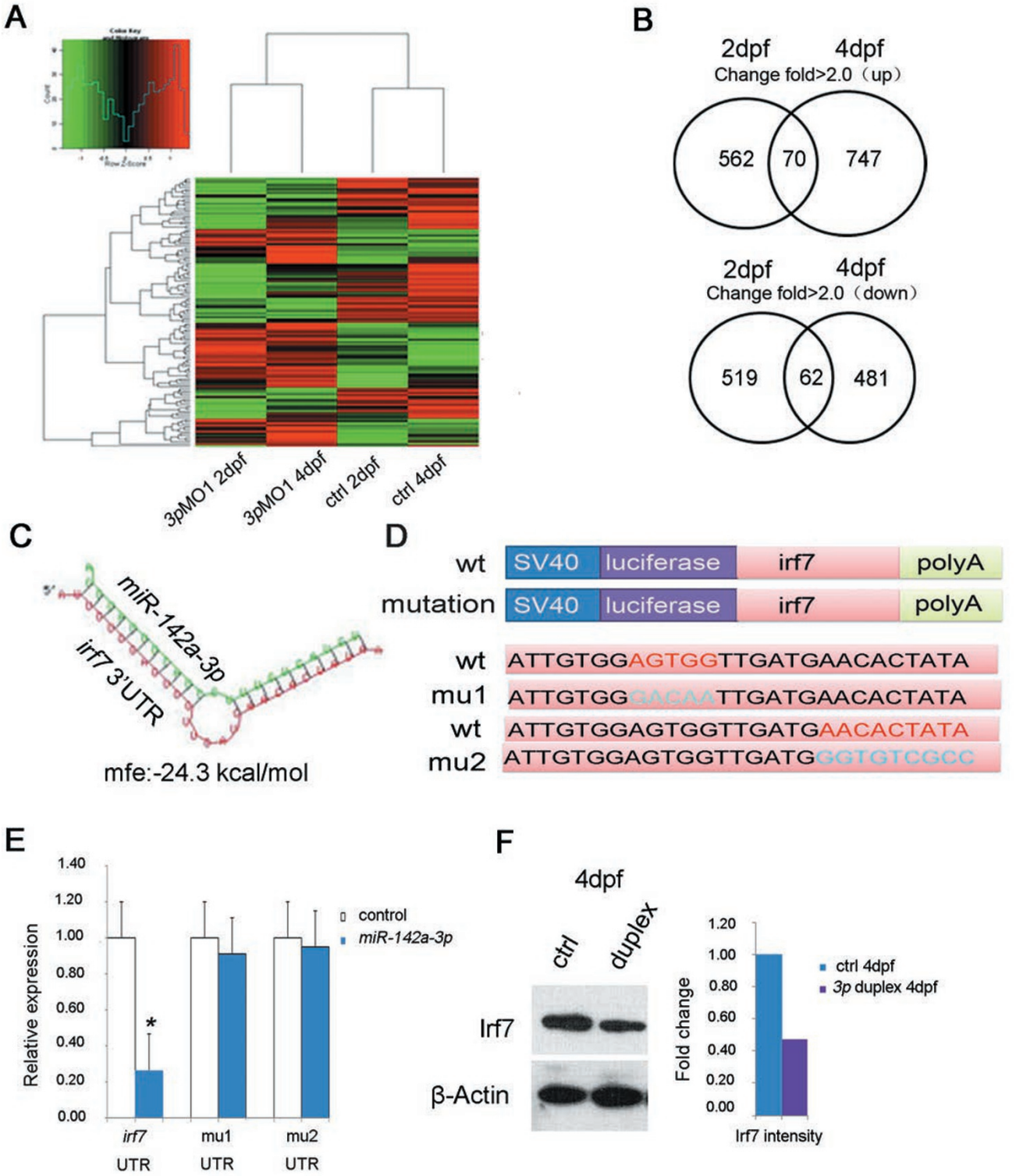

Figure 4 *irf7* is a direct target of *miR-142a-3p*. **(A)** Heat map analysis of gene expression in controls and *miR-142a-3p* morphants at 2 dpf and 4 dpf. **(B)** Fold changes of upregulated or downregulated genes at 2 dpf and 4 dpf in *miR-142a-3p* morphants compared to controls. **(C)** An imperfect match of *irf7* 3′ UTR with *miR-142a-3p* as determined by a calculation using RNAHybrid. **(D)** Scheme of the PGL3 constructs containing *irf7* WT and mutated 3′ UTR. **(E)** Luciferase reporter activity of the reporter containing WT or mutated *irf7* 3′ UTR when co-transfected with the *miR-142a-3p* duplex into HEK293T cells (mean ± SD, *t*-test, $*P < 0.05$, $n = 3$). **(F)** Western blotting images showing that *irf7* protein level was decreased in duplex-injected embryos at 4 dpf, compared to controls (left panel). Quantitative analysis of the western blotting results is shown in right panel.

To determine whether *irf7* is responsible for the *miR-142a-3p* morphant phenotypes, we employed a double-knockdown approach. Importantly, double knockdown by co-injecting *irf7* MO and *3p* MO1 partially rescued the expression of *runx1* at 24 hpf and that of *cmyb* at 36 hpf (Figure 5A). Furthermore, the double knockdown of *miR-142a-3p* and *irf7* clearly rescued the expression of the T-cell marker *rag1* (Figure 5A), suggesting that *irf7* is required for *miR-142a-3p*-regulated lineage differentiation. Western blotting confirmed that co-injecting *irf7* MO with *3p* MO1 restored the Runx1 protein level at 24 hpf (Figure 5B), which provided further evidence for the rescue of defects in HSC development by knocking down *irf7* in the *miR-142a-3p* morphants.

Decreased Gcsfr-Nitric Oxide (NO) inflammation signaling might lead to defects in HSC development in the miR-142a-3p morphants

To elucidate the mechanism underlying the *miR-142a-3p*-mediated regulation of HSC formation and differentiation, we focused on the downstream events of *miR-142a-3p-irf7* axis. *irf7* is a member of the *irf* family, and *irf* members often function in host defense and inflammation [27-30]. An inflammation pathway might be involved in HSC and myeloid lineage differentiation in zebrafish [31, 32]. Very recently, Hall *et al*. [31] reported that infection-induced Gcsfr-NO signaling can enhance the expansion of the hematopoietic stem and progenitor cell compartment in zebrafish. To test whether this signaling was involved in the *miR-142a-3p*-mediated regulation of HSC development, we examined *gcsfr*, a very important upstream component in inflammation signaling. The expression of *gcsfr* in the CHT region at 36 hpf was downregulated in the *miR-142a-3p* morphants or the *irf7*-overexpressing embryos, and the decrease of *gcsfr* expression in the *miR-142a-3p* morphants was partially rescued by co-injection of *irf7* MO (Figure 6A), suggesting that *gcsfr* acts downstream of *irf7*. The DAF-FM assay [33] showed that NO production was decreased in the *miR-142a-3p* morphants but was restored by co-injection of *irf7* MO (Figure 6B). NO production is also regulated by blood flow-induced Klf2a-eNOS signaling, as we reported previously [34]. To test whether blood flow-induced Klf2a signaling is involved in the defects in HSC development in the *miR-142a-3p* morphants, we evaluated the expression of *klf2a*. *klf2a* expression was not altered in the *miR-142a-3p* morphants compared to control embryos (Figure 6C), suggesting that *klf2a*-mediated blood flow did not contribute to the defects in HSC development in *miR-142a-3p* morphants. In addition, we also employed the rescue approach by treating *miR-142a-3p* morphants with the Gcsfr downstream NO agonist, S-nitroso N-acetylpenicillamine (SNAP). WISH showed that the expression of *runx1* in the AGM was partially restored by treating *miR-142a-3p* morphants with SNAP (Figure 6D). As expected, an injection of *gcsf* mRNA can also rescue the expression of *runx1* in *miR-142a-3p* morphants (Figure 6D). Taken together, these data suggest that *miR-142a-3p* regulates HSC formation and differentiation, at least in part, through Gcsfr-NO signaling.

miR-142-3p is involved in definitive hematopoiesis in mouse

Because the sequence of *miR-142-3p* is highly conserved in all vertebrates, including mammals (Supplementary information, Figure S1A), we hypothesized that *mmu-miR-142-3p*, the mouse homolog of *miR-142-3p*, might also function in the development of the HSCs in the AGM region of mouse embryos. To test this possibility, we first examined its expression in the mouse AGM region. The qPCR results clearly showed that *miR-142-3p* was highly expressed in E11.5 AGM tissues, but it was not detectable in the neighboring non-AGM tissues (Figure 7A).

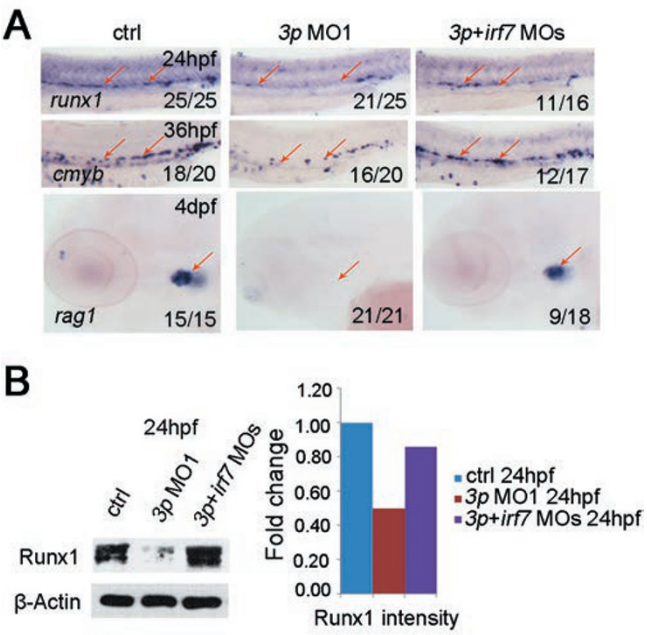

Figure 5 *irf7* knockdown can restore the expression of the HSC gene *runx1* and T-cell gene *rag1* in *miR-142a-3p* morphants. **(A)** *irf7* knockdown restores the expression of HSC genes *runx1* (24 hpf) and *cmyb* (36 hpf), and the T-cell marker *rag1* (4 dpf) in *miR-142a-3p* morphants, as determined by WISH. **(B)** *irf7* knockdown restores *runx1* expression at the protein level, as shown by western blotting (left panel) and quantitative analysis of the western blotting results (right panel).

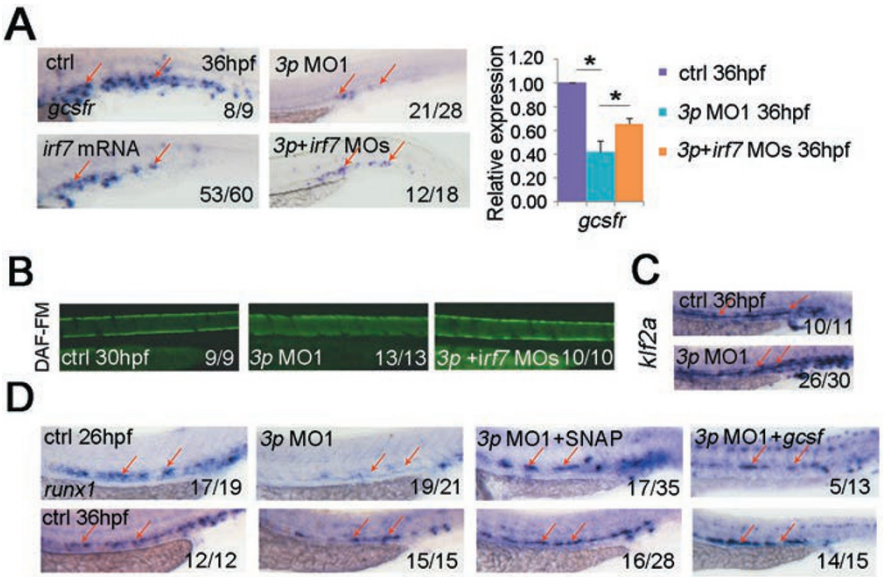

Figure 6 Decreased Gcsfr-NO inflammation signaling might lead to defects in HSC development in *miR-142a-3p* morphants. **(A)** Decreased expression of *gcsfr* in *miR-142a-3p* morphants and embryos injected with *irf7* mRNA at 36 hpf. Co-injection of the *irf7* MO partially rescued the *gcsfr* expression in *miR-142a-3p* morphants. Left panel, WISH; the red arrows indicate HSCs in the CHT region. Right panel, qPCR showing *gcsfr* expression in embryos injected with *3p* MO1 alone or in combination with *irf7* MO (mean ± SD, *t*-test, **P* < 0.05, *n* = 3). **(B)** DAF-FM assay performed at 30 hpf showed the decreased production of NO in *miR-142a-3p* morphants and its restoration by co-injection of *irf7* MO. **(C)** *klf2a* expression was unaffected in *miR-142a-3p* morphants at 36 hpf. **(D)** Partial rescue of *runx1* expression was achieved by treating *miR-142a-3p* morphants with the NO agonist SNAP or by injecting *gcsf* mRNA. The red arrows indicate *runx1* expression in the AGM region.

To determine the functional role of *miR-142-3p* in the HSCs of mouse embryos, we first performed a colony-forming unit-cell (CFU-C) assay *in vitro*. E11.5 AGMs (41-45 sp) were dissociated using collagenase and the cells were treated with the *miR-142-3p* duplex (20 pmol) or the *miR-142-3p* inhibitor (40 pmol). Then, the c-Kit$^+$CD34$^+$ cells were sorted and the indicated numbers of single cells were transferred to ultra-low attachment 24-well plates and cultured in CFU-C media. The cells were cultured for 7 days, and based on morphology, the colonies were categorized into BFU-E (burst forming unit-erythroid), CFU-GM (colony forming unit-granulocyte, macrophage), and mixed CFU-GEMM (colony forming unit-granulocyte, erythroid, macrophage, megakaryocyte) or CFU-Mix. We counted the colonies in each category, and found that the addition of the *miR-142-3p* inhibitor led to a 25% reduction of the total number of colonies, whereas the *miR-142-3p* duplex caused an approximately 2-fold increase of total colony number (Figure 7B). The proportions of each colony category showed little changes after either treatment (Figure 7B). To confirm the *in vitro* result, we performed a CFU-S (colony-forming unit-spleen) assay *in vivo*. As shown in Figure 7C, the number of CFU-S was increased in mice infused with duplex-treated AGM cells, whereas it was decreased in mice infused with inhibitor-treated AGM cells. These data suggest that *miR-142-3p* is important for the expansion of HSCs and their differentiation into lineage-restricted progenitors, such as erythroid and myeloid lineages, both *in vitro* and *in vivo*.

To determine whether *miR-142-3p* is also required for the differentiation of the T-lymphoid lineage in mouse, we performed a T-cell differentiation assay *in vitro* [35]. Dissociated cells from the AGM region were treated with the duplex or inhibitor for 5 h. Then, the sorted c-Kit$^+$CD34$^+$ cells were co-cultured with OP9-DL1 stromal cells and cytokines for 13 days, and the CD25$^+$CD44$^+$ T-cell progenitors were quantified by fluorescence-activated cell sorting (FACS). The results showed that the duplex increased, whereas the inhibitor decreased, the number of CD25$^+$CD44$^+$ cells (Figure 7D), indicating that *miR-142-3p* is required for T-cell differentiation. To investigate whether the expression of *irf7* is also negatively regulated by *miR-142-3p* in mouse, we performed qPCR to quantify the level of *irf7* expression after up- or down-regulation of *miR-142-3p* expression. As shown in Figure 7E, the mRNA level of *irf7* was decreased after *miR-142-3p* overexpression, whereas it was increased after the inhibition of *miR-142-3p* expression in c-Kit$^+$CD34$^+$ cells, which were dissociated from the E11.5

AGM and co-cultured with OP9 stromal cells for 48 h. Taken together, these results confirm the hypothesis that *miR-142-3p* is involved in the formation and differentiation of HSCs in the AGM of mouse embryos both *in vitro* and *in vivo*, suggesting a highly conserved role of *miR-142-3p* in definitive hematopoiesis in vertebrates, from zebrafish to mouse.

Discussion

Our study reveals that *miR-142-3p* plays pivotal roles in regulating the formation and lineage differentiation of

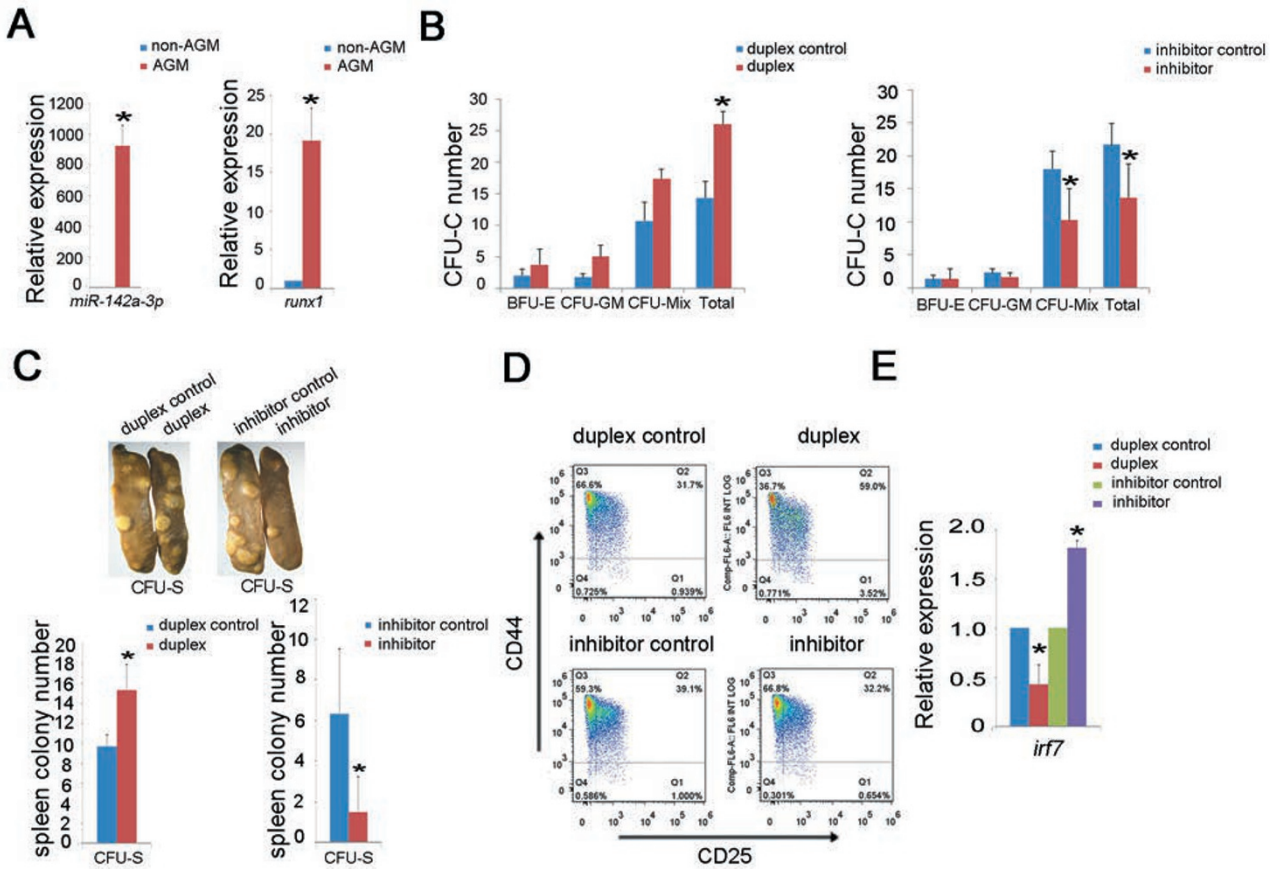

Figure 7 The involvement of *miR-142-3p* in HSC development in mouse. **(A)** Expression of *mmu-miR-142-3p* in dissected E11.5 AGM tissues and neighboring non-AGM tissues was determined by qPCR (mean ± SD, *t*-test, **P* < 0.05, *n* = 3). *runx1* was used as a positive control. **(B)** CFU-C assay. Isolated E11.5 AGM cells were transfected with the *miR-142-3p* duplex or inhibitor. Five hours after the transfection, the c-Kit$^+$CD34$^+$ cells were sorted, and cultured in CFU-C media for 7 days, and several types of colonies formed, including BFU-E, CFU-GM, and CFU-Mix colonies. The *mmu-miR-142-3p* duplex promoted colony formation, whereas the *mmu-miR-142-3p* inhibitor repressed colony formation. The colonies starting from a seeding density of 800 cells were counted to determine the CFU-C number. Data are presented as mean ± SD; **P* < 0.05. **(C)** CFU-S assay. The *in vivo* splenic colony assay showed that the CFU-S colony number was increased by ~1.5-fold after the transplantation of duplex-treated cells. However, the number decreased by ~3-fold after the transplantation of inhibitor-treated cells. Data are presented as mean ± SD; **P* < 0.05. **(D)** T-cell differentiation was assessed using FACS. The dissociated cells from the AGM region were treated with the duplex or the inhibitor for 5 h. Then, the sorted c-Kit$^+$CD34$^+$ cells were cultured under T-cell differentiation conditions. The T-lymphoid potential was determined by measuring CD44 and CD25 expression using FACS after 13 days of co-culture with OP9-DL1 cells. The number of lymphoid progenitors increased after duplex treatment while it decreased after inhibitor treatment (duplex control 39 ± 7%, duplex 53 ± 6%; inhibitor control 45.5 ± 7%, inhibitor 38.6 ± 6%) (*n* = 3, *P* < 0.05). **(E)** The expression of *irf7* was decreased in c-Kit$^+$CD34$^+$ cells by treatment with the *miR-142-3p* duplex, while it was increased by treatment with the inhibitor. A representative quantitative RT-PCR result showing the expression of *irf7* mRNA in *miR-142-3p* duplex- and inhibitor-treated c-Kit$^+$CD34$^+$ cells from the E11.5 AGM. Data are presented as mean ± SD; **P* < 0.05.

the earliest HSCs *in vivo* during vertebrate embryogenesis. We showed that *irf7* acts as a negative regulator of HSC development and differentiation into the T-cell lineages, which can be inhibited by *miR-142-3p*.

To date, very few miRNAs have been shown to play important roles in HSC development in vertebrates *in vivo*. *miR-142-3p* is specifically expressed in HSCs (AGM and CHT) and T cells (thymus) in zebrafish, mouse and other species [15-21]. By knockdown of *miR-142a-3p* using 2 specific MOs, the numbers of HSCs and T cells were decreased. Interestingly, a recent report using *miR-142*$^{-/-}$ mice also showed that more *miR-142*$^{-/-}$ CD4^{+} DCs underwent apoptosis than WT ones [36]. However, defects in HSC development were not examined in that study. Based on our present findings, we speculate that a similar phenotype would be observed at the onset of definitive hematopoiesis in *miR-142*$^{-/-}$ KO mice. Interestingly, a very recent report showed that in *Xenopus*, *miR-142-3p* is required for HSC lineage specification [37], which is consistent with the results for zebrafish and mouse embryos reported in this study. In contrast, an inverse correlation between *miR-142-3p* expression and HSC development has been suggested recently [20]. Bissels *et al*. [20] reported that overexpression of *miR-142-3p* at a dose of 50 nM in human CD133^{+} cells had a negative effect on their overall colony-forming ability. The apparent difference between those results and ours might be due to the source and age of the cells used (human bone marrow vs mouse AGM; 79 years vs E11.5) and the concentration of *miR-142-3p* utilized for overexpression (50 nM vs 20 pmol), which awaits further investigation.

Identifying the targets of *miR-142-3p* is crucial for analyzing the biological function of this miRNA during hematopoiesis. Among the four genes that we investigated, the expression of *irf7* was the most upregulated in *miR-142a-3p* morphants. Reporter assays and qPCR further indicated that *irf7* is a direct target of *miR-142a-3p*. More importantly, the *irf7* MO injection rescued the defects in HSC development and T-cell differentiation in the *miR-142a-3p* morphants. Members of the interferon regulatory factor (IRF) family of transcription factors mainly act as regulators of host defense and inflammation [27-30]. Inflammatory activation of early HSCs has been shown to be evolutionarily conserved [38], and a recent report by Hall *et al*. [31] demonstrated that, in zebrafish, Gcsfr-NO signaling is required for the expansion of HSCs following infection. Among the *irf* family members, *irf8* was shown to be required for myeloid differentiation into macrophages as opposed to neutrophils [39] and for the regulation of B-cell lineage specification and differentiation [40]. Here, we reveal that knocking down *miR-142a-3p* expression in zebrafish upregulated the expression of an *irf* family member, *irf7*, which might be responsible for the decreased HSC population in the *miR-142a-3p* morphants. We further showed that *irf7* is indeed a direct target of *miR-142a-3p*, which plays a pivotal role in regulating the formation and differentiation of HSCs in zebrafish *in vivo* and possibly also in mouse, at least *in vitro*. Further work is required to elucidate how *irf7* negatively regulates Gcsfr-NO signaling during HSC development under normal and stressful conditions. However, we cannot exclude the possibility that other target genes of *miR-142-3p* may also be involved in this process.

In summary, our results demonstrate that *miR-142-3p* regulates HSC development by directly targeting *irf7*. As *miR-142-3p* and *irf7* are highly conserved across species, the newly identified *miR-142-3p-irf7* axis provides new insights into miRNA modulation of HSC formation and differentiation in vertebrates and may provide new clues for the *in vitro* expansion of therapeutic HSCs.

Materials and Methods

Fish strains and embryos

Zebrafish embryos were obtained by the natural spawning of adult AB strain zebrafish. The embryos were raised and maintained at 28.5 °C in system water and staged as described previously [41]. The *fli1a*:EGFP [42] transgenic line was kindly provided by Steve Wilson (King's College London). The *cloche* carrier [43], *cmyb*:EGFP [26], and *kdrl*:mCherry/*cmyb*:EGFP [4] lines were kindly provided by Anming Meng (Tsinghua University). This study was approved by the Ethical Review Committee of the Institute of Zoology, Chinese Academy of Sciences, China.

MOs, duplex, mRNA synthesis and microinjection

Standard MOs and gene-specific antisense MOs were purchased from GeneTools (Philomath, OR) and prepared as 1 mM stock solutions using ddH_2O. The miRNA duplex was purchased from Invitrogen. mRNAs were synthesized using an Ambion mMessage mMachine kit (Ambion, Austin, TX). Standard MOs were used as negative controls in all of the MO injection experiments along with gene-specific MOs. For the fish embryo injections, MOs (2-10 ng), the duplex (5-20 pmol) and capped mRNA were injected separately or in combination into 1- to 2-cell-stage zebrafish embryos at the yolk/blastomere boundary. The MO sequences are listed in Supplementary information, Table S1.

WISH and cryosectioning

WISH of zebrafish embryos was performed as described previously [34] using probes for *myod*, *pax2.1*, *ccl25a*, *klf2a*, *ikaros*, *runx1*, *cmyb*, *dltc*, *flt4*, *foxn1*, *rag1*, *irf7*, *krt18*, *foxp1a*, *rxrab* and *gcsfr*. The LNA probe for *miR-142a-3p* was purchased from EXIQON. The WISH-labeled embryos were treated with 30% sucrose and then washed three times using PBST and embedded in O.C.T. medium (SAKURA). The embryos were sectioned using LEICA CM1900 cryostats.

Stem loop RT-PCR, quantitative RT-PCR and western blotting

The total RNA of embryos from the one-cell stage to 6 dpf was reverse-transcribed using the *miR-142a-3p* RT-primer 5′-GTCGTATCCAGTGCAGGGTCCGAGGTATTCGCACTGGATACGACTCCATA-3′, and the U6 RT primer 5′-AAAAATATGGAGCGCTTCACG-3′. Quantitative RT-PCR and western blotting were performed as described previously [34]. The PCR primers used are listed in Supplementary information, Table S2. All of the experiments were performed in at least triple duplicates in three different biological experiments. The data are given as mean ± SD. Student's *t*-test was used for statistical comparisons. $P < 0.05$ was considered significant and is indicated with one asterisk.

Zebrafish embryo dissociation and FACS

Embryo dissociation and FACS were performed as described previously by Covassin *et al*. [44]. The GFP^+ and GFP^- cells were separately collected from *cmyb*:EGFP and *runx1*:EGFP transgenic embryos (Zhang P and Liu F, unpublished data) using MoFlo XDP (Beckman). A plasmid containing a *runx1* intronic enhancer together with a heat-shock minimal promoter fused with EGFP was injected into embryos at the one-cell stage to generate a stable transgenic line.

Chemical treatment

Embryos at bud stage were treated with SNAP (Sigma-Aldrich) at the concentration of 10 μM. The treated embryos were examined periodically to ensure that the pharmacologic effect remained constant over time.

Confocal microscopy

Confocal images were acquired using a Zeiss LSM 510 META confocal laser microscope, and 3D projections were generated using Zeiss LSM software (Carl Zeiss Inc.).

Microarray assay

The total RNA was extracted from the AGM region of 2- and 4-dpf embryos using TRIzol (Tiangen, Beijing), and Cy3- or Cy5-labeled cDNAs from the controls and morphants were hybridized to Agilent Zebrafish Oligo Microarrays (Shanghai Biotechnology Co. Ltd., Shanghai). The expression data were subjected to hierarchical clustering and subsequently depicted in a heat map format.

Reporter assay

The WT and mutated *irf7* 3′ UTR were cloned and inserted into the *Eco*RI and *Spe*I sites of the pGL3-luciferase vector, which was kindly provided by Dr Peifeng Li (Institute of Zoology, CAS, Beijing, China). The mutation sites of *irf7* 3′ UTR were designed as follows: from WT 5′-AGTGG-3′ to mut1 5′-GACAA-3′ and from WT 5′-AACACTATA-3′ to mut2 5′-GGTGTCGCC-3′. WT or mutated pGL3-*irf7*-3′ UTR with or without the *miR-142a-3p* duplex (Invitrogen) were transfected into HEK293T cells using Lipofectamine 2000 (Invitrogen). The luciferase activity was measured using the luciferase activity assay kit (Promega).

DAF-FM assay

Embryos at 30 hpf were incubated with 5 μM DAF-FM diacetate (4-amino-5-methylamino-2′,7′-difluorofluorescein diacetate) for 2 h at 28.5 °C and then washed with fish water and observed under a fluorescence microscope.

CFU-C assay and quantitative RT-PCR

E11.5 mouse AGMs (41-45 sp) were dissociated using collagenase, and the cells were treated with the *miR-142-3p* duplex (Invitrogen) at 20 pmol and the inhibitor (Invitrogen) at 40 pmol. The procedures for siRNA transfection were performed as described in the Lipofectamine 2000 Transfection Reagent protocol (Invitrogen). After 5 h of transfection, antibody staining was performed for 30 min at 4 °C using antibodies specific for CD34 (BD) and c-Kit (eBioscience). The $c\text{-}Kit^+CD34^+$ cells were sorted using a MoFlo XDP (Beckman Coulter). The indicated numbers of single cells were transferred to ultra-low attachment 24-well plates (COSTAR) and cultured in CFU-C media. The cells were incubated at 37 ^oC in 5% CO_2 with 100% humidity for 7 days, and the number of each type of colony was counted according to their morphology. The experiment was repeated in triplicate. The sequences for the *miR-142-3p* inhibitor and duplex are listed in Supplementary information, Table S2.

After transfection with the *miR-142-3p* duplex or inhibitor, the FACS-sorted $c\text{-}Kit^+CD34^+$ cells were cultured on mouse OP9 stromal cells in medium supplemented with hematopoietic cytokines (50 ng/ml SCF, 10 ng/ml IL3, 10 ng/ml FL, 10 ng/ml IL-6, and 3 U/ml Epo). After being cultured for 48 h, the cells were harvested for quantitative PCR to evaluate the expression of *miR-142-3p* and *irf7*.

CFU-S assay

The AGM regions of E11.5 mouse embryos were dissected, and the cells were suspended as single cells in solution, and then were treated with the *miR-142-3p* duplex (20 pmol) or inhibitor (40 pmol). After 5 h transfection, one embryo equivalent was transplanted via the tail vein. There were four individual mice in each experimental group. The spleens were obtained 8 days posttransplantation, and the number of colonies formed was counted under a stereomicroscope.

T lymphoid progenitor differentiation assay

An equal number of $c\text{-}Kit^+CD34^+$ cells and OP9-DL1 stromal cells were co-cultured in α-MEM supplemented with 15% FBS, 50 ng/ml SCF, 10 ng/ml IL7, and 20 ng/ml FL-3. After 13 days of co-culture, the cells were labeled with CD25-PE and CD44-APC antibodies and analyzed using flow cytometry.

Statistical analysis

For statistical analysis, Student's unpaired two-tailed *t*-test was used for all of the comparisons unless otherwise indicated.

Acknowledgments

We thank the laboratory members for helpful discussions and critical reading of the paper. This work was supported by the National Basic Research Program of China (2010CB945300, 2011CB943900, and 2012CB945101), the National Natural Science Foundation of China (31271570, 90919055), and the Strategic Priority Research Program of the Chinese Academy of Sciences (XDA01010110).

References

1 Zhang C, Patient R, Liu F. Hematopoietic stem cell development and regulatory signaling in zebrafish. *Biochim Biophys Acta* 2013; **1830**:2370-2374.
2 Orkin SH, Zon LI. Hematopoiesis: an evolving paradigm for stem cell biology. *Cell* 2008; **132**:631-644.
3 Kissa K, Herbomel P. Blood stem cells emerge from aortic endothelium by a novel type of cell transition. *Nature* 2010; **464**:112-115.
4 Bertrand JY, Chi NC, Santoso B, *et al*. Haematopoietic stem cells derive directly from aortic endothelium during development. *Nature* 2010; **464**:108-111.
5 Bartel DP. MicroRNAs: genomics, biogenesis, mechanism, and function. *Cell* 2004; **116**:281-297.
6 Forman JJ, Coller HA. The code within the code: microRNAs target coding regions. *Cell Cycle* 2010; **9**:1533-1541.
7 O'Connell RM, Baltimore D. MicroRNAs and hematopoietic cell development. *Curr Top Dev Biol* 2012; **99**:145-174.
8 Bissels U, Bosio A, Wagner W. MicroRNAs are shaping the hematopoietic landscape. *Haematologica* 2012; **97**:160-167.
9 Lechman ER, Gentner B, van Galen P, *et al*. Attenuation of miR-126 activity expands HSC *in vivo* without exhaustion. *Cell Stem Cell* 2012; **11**:799-811.
10 Grabher C, Payne EM, Johnston AB, *et al*. Zebrafish microRNA-126 determines hematopoietic cell fate through c-Myb. *Leukemia* 2011; **25**:506-514.
11 Dore LC, Amigo JD, Dos Santos CO, *et al*. A GATA-1-regulated microRNA locus essential for erythropoiesis. *Proc Natl Acad Sci USA* 2008; **105**:3333-3338.
12 Fu YF, Du TT, Dong M, *et al*. Mir-144 selectively regulates embryonic alpha-hemoglobin synthesis during primitive erythropoiesis. *Blood* 2009; **113**:1340-1349.
13 Pase L, Layton JE, Kloosterman WP, *et al*. miR-451 regulates zebrafish erythroid maturation *in vivo* via its target gata2. *Blood* 2009; **113**:1794-1804.
14 Ramkissoon SH, Mainwaring LA, Ogasawara Y, *et al*. Hematopoietic-specific microRNA expression in human cells. *Leuk Res* 2006; **30**:643-647.
15 Chen CZ, Li L, Lodish HF, Bartel DP. MicroRNAs modulate hematopoietic lineage differentiation. *Science* 2004; **303**:83-86.
16 Reddy AM, Zheng Y, Jagadeeswaran G, *et al*. Cloning, characterization and expression analysis of porcine microRNAs. *BMC Genomics* 2009; **10**:65.
17 Liao R, Sun J, Zhang L, *et al*. MicroRNAs play a role in the development of human hematopoietic stem cells. *J Cell Biochem* 2008; **104**:805-817.
18 Jin P, Wang E, Ren J, *et al*. Differentiation of two types of mobilized peripheral blood stem cells by microRNA and cDNA expression analysis. *J Transl Med* 2008; **6**:39.
19 Sun W, Shen W, Yang S, *et al*. miR-223 and miR-142 attenuate hematopoietic cell proliferation, and miR-223 positively regulates miR-142 through LMO2 isoforms and CEBP-beta. *Cell Res* 2010; **20**:1158-1169.
20 Bissels U, Wild S, Tomiuk S, *et al*. Combined characterization of microRNA and mRNA profiles delineates early differentiation pathways of $CD133^+$ and $CD34^+$ hematopoietic stem and progenitor cells. *Stem Cells* 2011; **29**:847-857.
21 Yuan W, Sun W, Yang S, *et al*. Downregulation of microRNA-142 by proto-oncogene LMO2 and its co-factors. *Leukemia* 2008; **22**:1067-1071.
22 Wang XS, Gong JN, Yu J, *et al*. MicroRNA-29a and microRNA-142-3p are regulators of myeloid differentiation and acute myeloid leukemia. *Blood* 2012; **119**:4992-5004.
23 Sun Y, Varambally S, Maher CA, *et al*. Targeting of microRNA-142-3p in dendritic cells regulates endotoxin-induced mortality. *Blood* 2011; **117**:6172-6183.
24 Nishiyama T, Kaneda R, Ono T, *et al*. miR-142-3p is essential for hematopoiesis and affects cardiac cell fate in zebrafish. *Biochem Biophys Res Commun* 2012; **425**:755-761.
25 Lalwani MK, Sharma M, Singh AR, *et al*. Reverse genetics screen in zebrafish identifies a role of miR-142a-3p in vascular development and integrity. *PLoS One* 2012; **7**:e52588.
26 North TE, Goessling W, Walkley CR, *et al*. Prostaglandin E2 regulates vertebrate haematopoietic stem cell homeostasis. *Nature* 2007; **447**:1007-1011.
27 Ozato K, Tailor P, Kubota T. The interferon regulatory factor family in host defense: mechanism of action. *J Biol Chem* 2007; **282**:20065-20069.
28 Balaraman S, Tewary P, Singh VK, Madhubala R. Leishmania donovani induces interferon regulatory factor in murine macrophages: a host defense response. *Biochem Biophys Res Commun* 2004; **317**:639-647.
29 Fredericksen BL, Gale M Jr. West Nile virus evades activation of interferon regulatory factor 3 through RIG-I-dependent and -independent pathways without antagonizing host defense signaling. *J Virol* 2006; **80**:2913-2923.
30 Tamura T, Ozato K. ICSBP/IRF-8: its regulatory roles in the development of myeloid cells. *J Interferon Cytokine Res* 2002; **22**:145-152.
31 Hall CJ, Flores MV, Oehlers SH, *et al*. Infection-responsive expansion of the hematopoietic stem and progenitor cell compartment in zebrafish is dependent upon inducible nitric oxide. *Cell Stem Cell* 2012; **10**:198-209.
32 Liongue C, Hall CJ, O'Connell BA, Crosier P, Ward AC. Zebrafish granulocyte colony-stimulating factor receptor signaling promotes myelopoiesis and myeloid cell migration. *Blood* 2009; **113**:2535-2546.
33 North TE, Goessling W, Peeters M, *et al*. Hematopoietic stem cell development is dependent on blood flow. *Cell* 2009; **137**:736-748.
34 Wang L, Zhang P, Wei Y, *et al*. A blood flow-dependent klf2a-NO signaling cascade is required for stabilization of hematopoietic stem cell programming in zebrafish embryos. *Blood* 2011; **118**:4102-4110.
35 Li Z, Lan Y, He W, *et al*. Mouse embryonic head as a site for hematopoietic stem cell development. *Cell Stem Cell* 2012; **11**:663-675.
36 Mildner A, Chapnik E, Manor O, *et al*. Mononuclear phagocyte miRNome analysis identifies miR-142 as critical regulator of murine dendritic cell homeostasis. *Blood* 2013; **121**:1016-1027.
37 Nimmo R, Ciau-Uitz A, Ruiz-Herguido C, *et al*. miR-142-3p controls the specification of definitive hemangioblasts during ontogeny. *Dev Cell* 2013; **26**:237-249.
38 Takizawa H, Boettcher S, Manz MG. Demand-adapted regulation of early hematopoiesis in infection and inflammation.

Blood 2012; **119**:2991-3002.
39 Li L, Jin H, Xu J, *et al*. Irf8 regulates macrophage versus neutrophil fate during zebrafish primitive myelopoiesis. *Blood* 2011; **117**:1359-1369.
40 Wang H, Lee CH, Qi C, *et al*. IRF8 regulates B-cell lineage specification, commitment, and differentiation. *Blood* 2008; **112**:4028-4038.
41 Kimmel CB, Ballard WW, Kimmel SR, Ullmann B, Schilling TF. Stages of embryonic development of the zebrafish. *Dev Dyn* 1995; **203**:253-310.
42 Lawson ND, Weinstein BM. *In vivo* imaging of embryonic vascular development using transgenic zebrafish. *Dev Biol* 2002; **248**:307-318.
43 Stainier DY, Weinstein BM, Detrich HW III, *et al*. Cloche, an early acting zebrafish gene, is required by both the endothelial and hematopoietic lineages. *Development* 1995; **121**:3141-3150.
44 Covassin L, Amigo JD, Suzuki K, *et al*. Global analysis of hematopoietic and vascular endothelial gene expression by tissue specific microarray profiling in zebrafish. *Dev Biol* 2006; **299**:551-562.

(**Supplementary information** is linked to the online version of the paper on the *Cell Research* website.)